http://dx.doi.org/10.5012/bkcs.2014.35.11.3294

Coherent Control of Autler-Townes Splitting in Photoelectron Spectroscopy: The Effect of Laser Intensity and Laser Envelope

Chaochao Qin,* Hongsheng Zhai, Xianzhou Zhang, and Yufang Liu

Department of Physics, Henan Normal University, Xinxiang 453007, People's Republic of China.
**E-mail: qinch@hotmail.com*
Received March 2, 2014, Accepted July 29, 2014

We theoretically investigated the coherent control of Autler-Townes splitting in photoelectron spectroscopy of K_2 molecule within an ultrafast laser pulse by solving the time-dependent Schrodinger equation using a quantum wave packet method. It was theoretically shown that we can manipulate the splitting of photoelectron spectroscopy by altering the laser intensity. Furthermore, it was found that the percentages of each peak in photoelectron spectroscopy can be controlled by changing the envelope of the laser pulse.

Key Words : Coherent control, Photoelectron spectroscopy, Split-operator method

Introduction

With the rapid development of ultrafast laser pulse technology, many interesting phenomena have been investigated and discovered both theoretically and experimentally, including above threshold ionization and dissociation,[1,2] the laser control of molecular alignment and orientation,[3,4] the generation of attosecond pulses,[5] and dynamic Stark control of photochemical processes.[6] The relevant laser parameters, such as intensity, width and shape of pulse, have been used to control the molecular excitation, dissociation and ionization.

When the transition between two quantum levels is driven strongly with a resonant drive field, the resulting 'dressed' system can be equivalently viewed as two split levels, with splitting equal to the Rabi frequency of the drive field. This splitting can be observed spectroscopically by probing transitions to a third level in the system, which comprises the Autler–Townes (AT) effect. Autler-Townes splitting of atomic system has been observed for a long time.[7] In recent years, the ac-Stark effect and the AT splitting in gas-phase molecules have also been investigated.[8] Quesada *et al.* reported that one can obtain the transition dipole moment of H_2 molecules from the measurement of the AT splitting.[9] Qi *et al.* pointed out that AT splitting induced by CW pulse can be used as a way to facilitate all-optical control of molecular angular momentum alignment.[10,11] Sun and Lou demonstrated that one can observe the AT splitting in the photoelectron spectrum of a two-level Na_2 system with a proper ultrashort laser pulse.[12] Hu *et al.* studied theoretically this kind of AT splitting in the photoelectron spectrum for a Li_2 molecular system using one-dimension wave packet method.[13] But because of the relatively small value of the typical molecular transition dipole moment and rigorous requirement for laser pulses, the experimental observation and coherent control of AT splitting in a molecular system caused by femtosecond laser pulses has been hardly ever reported.

In the present work, we theoretically investigate the coherent control of AT splitting in the photoelectron spectroscopy of K_2 molecules by solving the time-dependent Schrodinger equation using a quantum wave packet method. We demonstrate that we can manipulate the splitting and the percentages of each peak in photoelectron spectrum by changing the laser intensity and the laser envelope.

Theoretical Method

Our numerical simulations include four electronic states[14-18], the ground state $X^1\Sigma_g^+$ the two excited states $A^1\Sigma_g^+$ and $2^1\Pi_g^+$, and the ionic ground state $X^2\Sigma_g^+$, as shown in Figure 1. For convenience, we refer to the four electronic states as $|0\rangle$, $|1\rangle$, $|2\rangle$, and $|I\rangle$, respectively. The rotational degree of freedom is neglected in our treatment because rotational motion of K_2 molecules is almost frozen in femtosecond time scale. Under the Born-Oppenheimer approximation, the wavefunction $\psi(R, t)$ can be obtained by solving the time-dependent Schrödinger equation

$$i\hbar\frac{\partial}{\partial t}\psi(R,t) = \hat{H}\psi(R,t)\,. \tag{1}$$

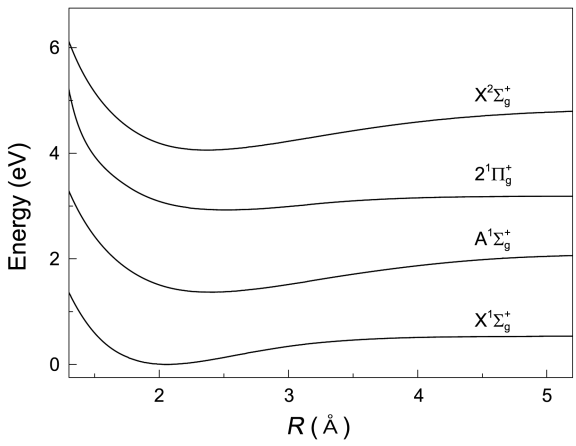

Figure 1. Relevant potential energy curves of K_2 used in this work.[14-18]

where $\hat{H}$ is the time-dependent Hamiltonian including the laser-molecule interaction, R is the internuclear separation. The molecular wavefunction $\psi(R, t)$ can be expressed as

$$\psi(R,t) = \sum_a \chi_a(R,t)|a\rangle + \int dE\chi_1(R,t)|E\rangle, \quad (2)$$

where a = 0, 1, and 2 are the three bound states, and $\chi_I(R, t)$ is the wavefunction of ionic state.

The ionization continuum is discretized into a band of quasicontinuum levels in terms of electron eigenstates $|E\rangle$ containing the core and free electron.[19] The states are labeled according to kinetic energy of the ejected electron:

$$\psi_I(R,t) = \sum_{n=1}^{N} \chi_I^n(R; E_n, t)|E_n\rangle, \quad (3)$$

where E_1 and E_n are the smallest and largest energy which can be transferred to the ejected electron, respectively. $\chi_I^n(R; E_n, t)$ are the nuclear wavefunction of K_2^+ corresponding to the emission of an electron with kinetic energy E_n. This leads to a Hamiltonian matrix of $(N+3)*(N+3)$ dimensions, including three bound states and N ionization quasicontinuum states. In the present work, N is chosen to be 241, E_1 and E_n are taken as 0 and 1.2 eV, respectively. Thus, Eq. (1) can be rewritten as

$$i\hbar\frac{\partial}{\partial t}\begin{pmatrix}\chi_0\\ \chi_1\\ \chi_2\\ \chi_I^1\\ \vdots\\ \chi_I^N\end{pmatrix} = \begin{pmatrix} H_{00} & W_{01} & 0 & 0 & \cdots & 0\\ W_{10} & H_{11} & W_{12} & 0 & \cdots & 0\\ 0 & W_{21} & H_{22} & W_{2I} & \cdots & W_{2I}\\ 0 & 0 & W_{12} & H_{II}^1 & \cdots & \\ \vdots & \vdots & \vdots & \vdots & \ddots & \\ 0 & 0 & W_{12} & 0 & \cdots & H_{II}^N \end{pmatrix}\begin{pmatrix}\chi_0\\ \chi_1\\ \chi_2\\ \chi_I^1\\ \vdots\\ \chi_I^N\end{pmatrix}. \quad (4)$$

The diagonal elements can be expressed as

$$H_{ii} = -\frac{\hbar^2}{2m}\frac{d^2}{dR^2} + V_i(R). \quad (5)$$

where m is the reduced mass of K_2 molecules, and $V_i(R)$ including the bound and quasicontinuum states are potential matrix elements of molecule in the absence of laser fields. In the dipole approximation, the matrix elements describing the laser-molecule interaction can be written as

$$\begin{aligned} W_{10} &= W_{01} = -\mu_{10}(R)\varepsilon(t),\\ W_{21} &= W_{12} = -\mu_{21}(R)\varepsilon(t),\\ W_{I2} &= W_{2I} = -\mu_{I2}(R)\varepsilon(t), \end{aligned} \quad (6)$$

where μ_{10}, μ_{21}, and μ_{I2} represent the transition dipole moments[20,21] between different electronic states and $\varepsilon(t)$ denotes the laser fields which are given by

$$\varepsilon(t) = \varepsilon_0 f(t)\cos(\omega t), \quad (7)$$

where ε_0 the is peak intensity, $f(t)$ is the pulse envelope and the center frequency of the ultrashort laser pulse ω is set to be 12 739 cm^{-1}, corresponding to the laser centre wavelength of 785 nm.

The time-dependent populations of the state is calculated by

$$P(t) = \int |\psi_i(R, t)|^2 dR. \quad (8)$$

The photoelectron spectroscopy is defined as

$$P(E_n) = \lim_{t\to\infty} \int |\psi_I(R; E_n, t)|^2 dR. \quad (9)$$

Results and Discussion

The initial wavefunction of the ground vibrational states of the $|0\rangle$ state is obtained by using the Fourier Grid Hamiltonian (FGH) method.[22-24] The propagation of wavefunction $\psi(R, t)$ is accomplished by employing the split-operator method.[25-27]

Figure 2 displays the photoelectron spectroscopy of K_2 calculated within the quantum wave packet model mentioned above, where the envelope of laser pulse is chosen to be a Gaussian function ($f(t) = \exp[-2\ln2(t/\tau)^2]$), the full width at half maximum (FWHM) of the laser pulse τ is 20 fs and the peak intensity is 5.0×10^{11} W/cm^2. We find that the photoelectron spectrum consists of three peaks centered at about 0.30 eV, 0.51 eV and 0.73 eV, which corresponding to slow-energy (S), medium-energy (M) and fast-energy (F) photoelectrons, respectively. It is obviously that the splitting of photoelectron spectroscopy in Figure 2 are almost the same but the percentages of S, M and F photoelectrons are 3.9%, 35.3% and 60.7%, respectively.

The time evolution of the population of the states $|0\rangle$, $|1\rangle$ and $|2\rangle$ are shown in Figure 3(a), (b) and (c), respectively. There are obvious Rabi oscillation in the time evolution of the population of three states. The splitting pattern in the photoelectron spectrum can be regarded as the AT splitting, which comes from three strongly coupled coherent vibrational states evolving along their own molecular electronic potential curves (*i.e.*, the AT splitting is induced by sufficiently rapid Rabi oscillations shown in Fig. 3). Since the motion associated with the molecular vibration is quite slow on the

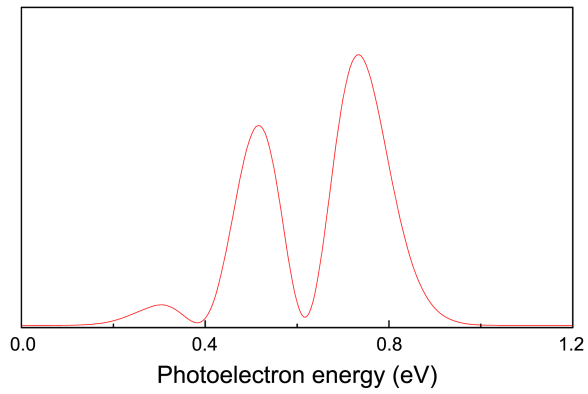

Figure 2. The photoelectron spectroscopy of K_2 for the Gaussian pulse, the full width at half maximum (FWHM) of the laser pulse τ is 20 fs and the peak intensity is $5I_0$ ($I_0 = 1.0 \times 10^{11}$ W/cm^2).

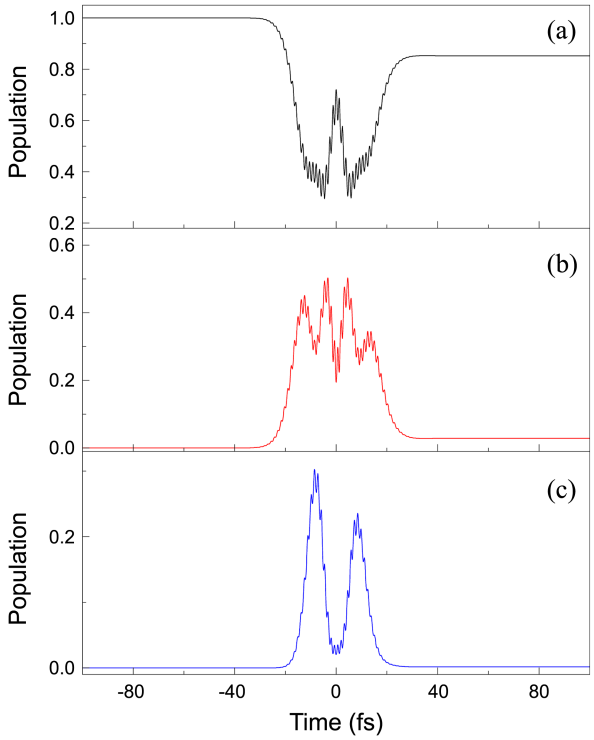

Figure 3. The time evolution of the population of the state (a) $|0\rangle$, (b) $|1\rangle$ and (c) $|2\rangle$.

field-molecule interaction time scale, the excited wave packets on the electronic $|1\rangle$ and $|2\rangle$ states don't move from the initial region where they are resonantly coupled by laser fields. The resonant region ΔR is located near the equilibrium position R_0 in the electronic ground state where $\hbar\omega$ equals the energy difference between the potentials of the three electronic states. Therefore, the process of the field-molecule interaction can be regarded as that of a three-level filed-atom interaction, and the corresponding levels are of $X^1\Sigma_g^+$, $A^1\Sigma_g^+$ and $2^1\Pi_g^+$, respectively. In term of the traditional explanation of ac-Stark splitting in dressed stated picture, the three-peak structure should arise from the sufficient Rabi oscillation between three intermediate resonant states during the ionization process.

Next, we consider the case of K_2 molecule driven by the different intensities of laser pulse. Figure 4 displays the photoelectron spectra as a function of the laser intensity I for the centre wavelength λ = 785 nm. We find that the position of these three peaks are good agreement with the straight lines shown in Figure 4, which corresponding to the functional expression $E_i = 0.51, 0.51 \pm \varepsilon_0\sqrt{\mu_{10}^2(R_0)+\mu_{21}^2(R_0)}/2\hbar$. At the laser intensity of $3I_0$, the S, M, and F photoelectrons are situated at 0.36 eV, 0.51 eV and 0.68 eV, and the percentages of S, M and F photoelectrons in the photoelectron spectrum are 4.9%, 34.1% and 61.0%, respectively. When the laser intensity increase to $7I_0$, the S, M, and F photoelectrons are situated at 0.26 eV, 0.51 eV and 0.78 eV, and the percentages of S, M and F photoelectrons in the photoelectron spectrum are corresponding to 3.7%, 30.5% and 65.8%, respectively. We conclude that the intensity of laser pulse varies from 3 I_0 to 7 I_0, there are fewer effects on the percentages of S, M and F photoelectrons, but the positions of S and F photoelectrons are shifted by about 0.1 eV. From the intuitive physical picture of the observed photoelectron spectra shown in Figure 4, we could directly deduce the energies and populations of the dressed states $|\alpha\rangle$, $|\beta\rangle$ and $|\gamma\rangle$, which corresponding to the S, M and F photoelectrons in the photoelectron spectrum, respectively. Compared to the "bare" state $|2\rangle$, the energies of dressed states $|\alpha\rangle$, $|\beta\rangle$ and $|\gamma\rangle$ are shifted about $\varepsilon_0\sqrt{\mu_{10}^2(R_0)+\mu_{21}^2(R_0)}/2\hbar$, 0 and $-\varepsilon_0\sqrt{\mu_{10}^2(R_0)+\mu_{21}^2(R_0)}/2\hbar$,

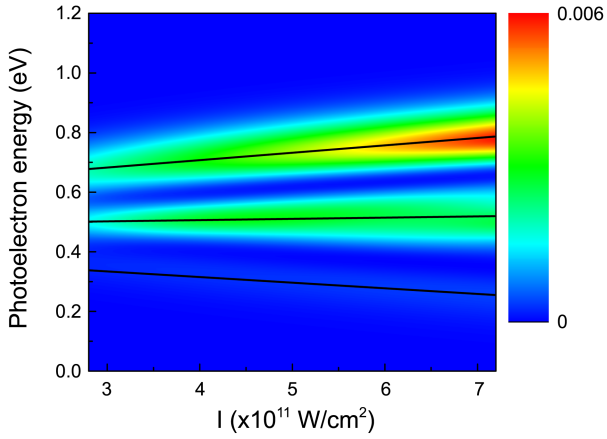

Figure 4. The photoelectron spectra of K_2 molecule as a function of laser intensity I. The other parameters of the laser pulse are same as that used in Figure 2.

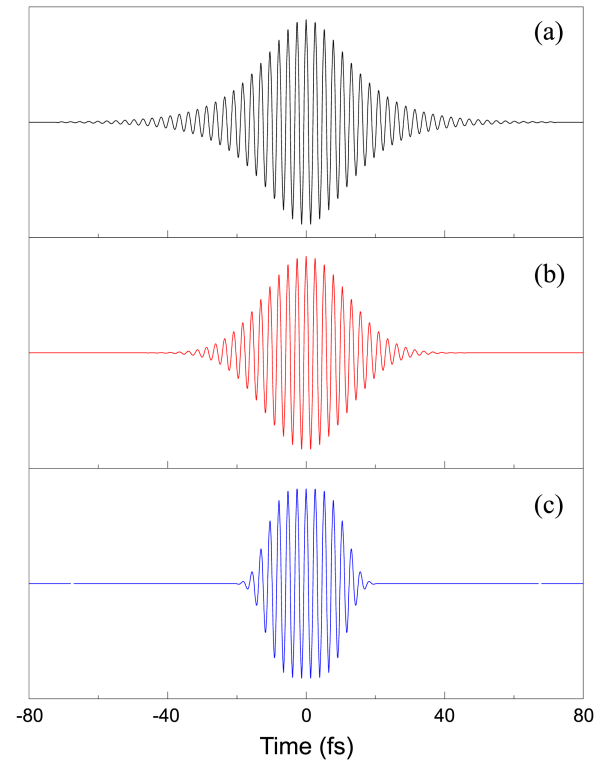

Figure 5. The electric field profile for (a) Secant, (b) Gaussian and (c) super-Gaussian laser pulse, the full width at half maximum (FWHM) of the laser pulse τ is 20 fs and the peak intensity is 5.0 × 10^{11} W/cm^2.

respectively. The ratio of dressed states populations on $|\alpha\rangle$, $|\beta\rangle$ and $|\gamma\rangle$ states is almost unchanged as the laser intensity varies from $3I_0$ to $7I_0$. Thus, we can manipulate the dressed states energies without changing the selective population of dressed states. Moreover, the AT splitting can be used to determine the *R*-dependent effective molecular transition dipole moment or the peak intensity of laser filed.

Furthermore, we consider the case of the K_2 molecule driven by different pulse shapes. Here, we adopt three different envelopes: Secant ($f(t) = \mathrm{sech}[2\ln(1+2^{1/2})t/\tau]$), Gaussian ($f(t) = \exp[-2\ln2(t/\tau)^2]$) and super-Gaussian ($f(t) = \exp[-8\ln2(t/\tau)^4]$).The electric field profile of the three pulses are shown in Figure 5(a), Figure 5(b) and Figure 5(c), respectively. The full width at half maximum (FWHM) and the peak intensity of the three laser pulse are same as that used in Figure 2. The corresponding calculated photoelectron spectrum are shown in Figure 6(a), Figure 6(b) and Figure 6(c), respectively. When the pulse envelope f(t) takes the Secant form, the right peak is the highest one, the S, M, and F photoelectrons are situated at 0.30 eV, 0.51 eV and 0.78 eV, and the percentages of S, M and F photoelectrons in the photoelectron spectrum are corresponding to 0.9%, 16.9% and 82.2%, respectively. Compared to that of the Gaussian form, the left peak and the medium peak are reduced and the right peak is enhanced. However, this situation is obviously changed for the super-Gaussian pulse: the medium peak becomes the highest one, the S, M, and F photoelectrons are situated at 0.28 eV, 0.51 eV and 0.75 eV, and the percentages of S, M and F photoelectrons in the photoelectron spectrum are corresponding to 15.0%, 50.4% and 34.6%, respectively.

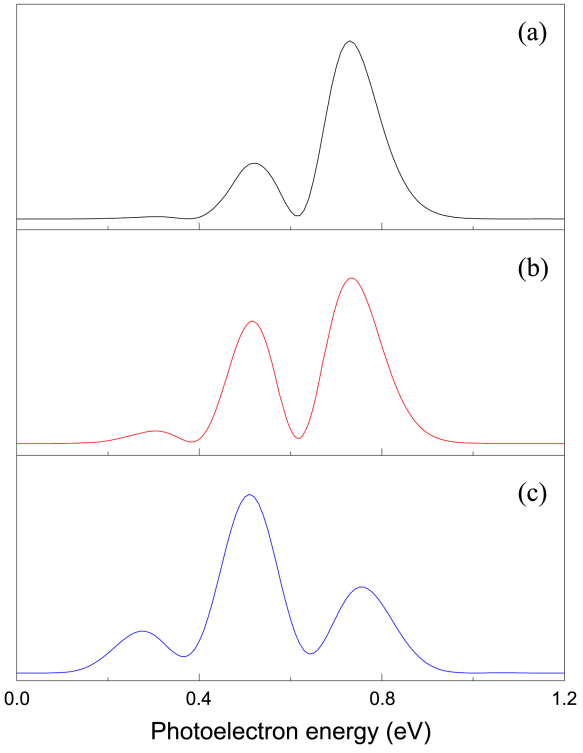

Figure 6. The corresponding photoelectron spectroscopy of K_2 for (a) Secant, (b) Gaussian and (c) super-Gaussian laser pulse.

Therefore, when we change the envelope of laser pulse varies from Secant to super-Gaussian, the percentages of S, M and F photoelectrons change a lot, but there are fewer effects on the positions of S, M and F photoelectrons. As mentioned above, the dressed states $|\alpha\rangle$, $|\beta\rangle$ and $|\gamma\rangle$ are corresponding to the S, M and F photoelectrons in the photoelectron spectrum, respectively. Thus, the populations on the dressed states are dependent on the pulse shape and we can steer the dressed states population without altering the energies of dressed states by changing the laser envelope.

Conclusion

In conclusion, the coherent control of photoelectron spectroscopy of K_2 molecule in an ultrafast laser pulse was theoretically investigated by using the quantum wave packet method. It was theoretically shown that the splitting of photoelectron spectrum can be controlled by changing the laser intensity. When the laser intensity varies from $3I_0$ to $7I_0$, the energies of S and F photoelectrons are shifted about 0.1 eV. In addition, the percentages of each peak of photoelectron spectrum can be manipulated by altering the envelope the laser pulse. When the envelope of the laser pulse vary from Secant to super-Gaussian, the percentages of the S and M photoelectron increase from 0.9% to 15.0% and 16.9% to 50.4%, respectively, but the F photoelectron decrease from 82.2% to 34.6%.

Acknowledgments. The author gratefully acknowledges the financial support from the National Natural Science Foundation of China (under Grant Nos. 11304157 and 11274096), the Basic and Advanced Technology Research Program of Henan Province (under Grant Nos. 142102310274 and 142300410168) and the Foundation for Key Program of Education Department of Henan Province (Grant No. 13A140519).

References

1. Quan, W.; Lin, Z.; Wu, M.; Kang, H.; Liu, H.; Liu, X.; Chen, J.; Liu, J.; He, X. T.; Chen, S. G.; Xiong, H.; Guo, L.; Xu, H.; Fu, Y.; Cheng, Y.; Xu, Z. Z. *Phys. Rev. Lett.* **2009**, *103*, 093001.
2. Orr, P. A.; Williams, I. D.; Greenwood, J. B.; Turcu, I. C. E.; Bryan, W. A.; Pedregosa-Gutierrez, J.; Walter, C. W. *Phys. Rev. Lett.* **2007**, *98*, 163001.
3. Stapelfeldt, H.; Seideman, T. *Rev. Mod. Phys.* **2003**, *75*, 543.
4. Holmegaard, L.; Nielsen, J. H.; Nevo, I.; Stapelfeldt, H.; Filsinger, F.; Kupper, J.; Meijer, G. *Phys. Rev. Lett.* **2009**, *102*, 023001.
5. Sansone, G.; Benedetti, E.; Calegari, F.; Vozzi, C.; Avaldi, L.; Flammini, R.; Poletto, L.; Villoresi, P.; Altucci, C.; Velotta, R.; Stagira, S.; De Silvestri, S.; Nisoli, M. *Science* **2006**, *314*, 443.
6. Sussman, B. J.; Townsend, D.; Ivanov, M. Y.; Stolow, A. *Science* **2006**, *314*, 278.
7. Autler, S. H.; Townes, C. H. *Phys. Rev.* **1955**, *100*, 703.
8. Xu, S.; Sha, G. H.; Jiang, B.; Sun, W. Z.; Chen, X. L.; Zhang, C. H. *J. Chem. Phys.* **1994**, *100*, 6122.
9. Quesada, M. A.; Lau, A. M. F.; Parker, D. H.; Chandler, D. W. *Phys. Rev. A* **1987**, *36*, 4107.
10. Qi, J.; Lazarov, G.; Wang, X.; Li, L.; Narducci, L. M.; Lyyra, A. M.; Spano, F. C. *Phys. Rev. Lett.* **1999**, *83*, 288.

11. Qi, J.; Spano, F. C.; Kirova, T.; Lazoudis, A.; Magnes, J.; Li, L.; Narducci, L. M.; Field, R. W.; Lyyra, A. M. *Phys. Rev. Lett.* **2002**, *88*, 173003.
12. Sun, Z.; Lou, N. *Phys. Rev. Lett.* **2003**, *91*, 023002.
13. Hu, W. H.; Yuan, K. J.; Han, Y. C.; Shu, C. C.; Cong, S. L. *Int. J. Quantum. Chem.* **2010**, *110*, 1224.
14. Jraij, A.; Allouche, A. R.; Magnier, S.; Aubert-Frecon, M. *Can. J. Phys.* **2008**, *86*, 1409.
15. Jraij, A.; Allouche, A. R.; Magnier, S.; Aubert-Frecon, M. *J. Chem. Phys.* **2009**, *130*, 244307.
16. Jong, G.; Li, L.; Whang, T. J.; Stwalley, W. C.; Coxon, J. A.; Li, M.; Lyyra, A. M. *J. Mol. Spectrosc*. **1992**, *155*, 115.
17. Broyer, M.; Chevaleyre, J.; Delacretaz, G.; Martin, S.; Woste, L. *Chem. Phys. Lett.* **1983**, *99*, 206.
18. Kowalczyck, P.; Kasahara, S.; Kabir, M. H.; Kato, H. *J. Mol. Spectrosc.* **2003**, *220*, 162.
19. Yuan, K. J.; Sun, Z. G.; Cong, S. L.; Lou, N. Q. *Phys. Rev. A* **2006**, *74*, 043421.
20. Vivie-Riedle, R. D.; Kobe, K.; Manz, J.; Meyer, W.; Reischl, B.; Rutz, S.; Schreiber, E.; Woste, L. *J. Phys. Chem.* **1996**, *100*, 7789.
21. Meng, Q. T.; Yang, G. H.; Sun, H. L.; Han, K. L.; Lou, N. Q. *Phys. Rev. A* **2003**, *67*, 043423.
22. Marston, C. C.; Balintkurti, G. G. *J. Chem. Phys.* **1989**, *91*, 3571.
23. Colbert, D. T.; Miller, M. H. *J. Chem. Phys.* **1991**, *96*, 1982.
24. Willner, K.; Dulieu, O.; Masnou-Seeuwsa, F. *J. Chem. Phys.* **2004**, *120*, 548.
25. Feit, M. D.; Fleck, J. A.; Steiger, A. *J. Comput. Phys.* **1982**, *47*, 412.
26. Kosloff, R. *J. Phys. Chem.* **1988**, *92*, 2087.
27. Chu, T. S.; Zhang, Y.; Han, K. L. *Int. Rev. Phys. Chem.* **2006**, *25*, 201.